SIRT5 promote malignant advancement of chordoma by regulating the desuccinylation of c-myc

Minghui Jiang[1†], Zheng Huang[2†], Li Chen[1], Ting Deng[1], Junpeng Liu[3] and Yue Wu[3,4*]

Abstract

Chordoma is a relatively rare and locally aggressive malignant tumor. Sirtuin (SIRT)5 plays pivotal roles in various tumors, but the role of SIRT5 in chordoma has not been found. This study was performed to investigate the regulatory effects of SIRT5 on cell proliferation, migration, and invasion and the underlying mechanism in chordoma. A xenograft tumor mouse model was established to assess tumor growth. Reverse transcription-quantitative polymerase chain reaction was used to analyze the mRNA levels of SIRT5 and c-myc. The effects of SIRT5 and c-myc on cell proliferation, migration, and invasion of chordoma cells were detected by cell counting kit-8, colony formation, and Transwell assays. The interaction between SIRT5 and c-myc was evaluated by co-immunoprecipitation (IP) assay. The succinylation of c-myc was analyzed by IP and Western blot. The results showed that SIRT5 expression was upregulated in chordoma tissues and cells. SIRT5 interacted with c-myc to inhibit the succinylation of c-myc at K369 site in human embryonic kidney (HEK)-293T cells. Silencing of SIRT5 suppressed the cell proliferation, migration, and invasion of chordoma cells, while the results were reversed after c-myc overexpression. Moreover, silencing SIRT5 suppressed tumor growth in mice. These findings suggested that SIRT5 promoted the malignant advancement of chordoma by regulating the desuccinylation of c-myc.

Keywords Chordoma, SIRT5, Desuccinylation, c-myc, Proliferation, Migration

[†]Minghui Jiang and Zheng Huang contributed equally to this work.

*Correspondence:
Yue Wu
wuyue1984110@163.com
[1]Department of Orthopedics, ChangSha Third Hospital, ChangSha, China
[2]Department of Orthopedics, HuaZhong University of Science and Technology Union Shenzhen Hospital, Shenzhen, China
[3]Department of Orthopedics, BeiJing ChaoYang Hospital, Beijing, China
[4]Department of Orthopedics, BeiJing ChaoYang Hospital, BeiJing Chao-Yang Hospital, No.8 Gongti South Rd, Chaoyang District, 100020 Beijing, China

Introduction

Chordoma, accounts for 1–4% of all bone tumors, is a primary, slowly growing, and locally aggressive neoplasms bone cancer that mainly affects the axial skeleton [1, 2]. Spinal residue, myelitis infection, and heredity are the main risk factors for chordoma induction. Chordoma can affect multiple sites of the axial skeleton, with 32% occurring inside the skull, 29.2% in the sacrum, and 32.8% affecting the rest of the spine [3]. Regrettably, about 30–40% of chordoma patients develop multiorgan (including liver, lung, and lymph nodes) metastasis [4]. For the treatment, chordoma is not sensitive to chemotherapy and is currently mainly treated with surgical resection and radiotherapy [5]. However, due to the complex and delicate structure of the central nervous system,

Jiang *et al. BMC Cancer*   (2024) 24:386

Page 2 of 10

appropriate surgical removal in clinical is difficult [6, 7]. Therefore, the prognosis for patients with chordoma remains poor, with more than 40% of patients experiencing postoperative recurrence [8]. Thus, molecular mechanisms and novel treatments for chordoma are worth further exploration.

The discovery of succinylation of lysine originates from the studies on acetylation [9]. In 2011, Zhang et al. identify succinylation modification as a new posttranslational modification (PTM) [10]. Over the next decade, succinylation modification was studied extensively on different diseases. Nowadays, succinylation is considered as a PTM widely present in prokaryotes and eukaryotes, and plays vital roles in regulating various physiological or pathological functions including signaling pathways, mitochondrial metabolism, and energy metabolism [11]. Succinylation works by regulating the structure of the protein by transferring the succinyl group ($-CO-CH_2-CH_2-CO_2H$) to the residue of the target protein [12]. Interestingly, the effects of succinylation on the structure and function of target proteins may be greater than that of other PTMs [12]. Previous studies have demonstrated the role of succinylation in various diseases, including cancers [13–15]. In addition, the degree of succinylation of certain proteins is regulated by the desuccinylation process. Sirtuin (SIRT)5 is the only known desuccinylase, located in the mitochondria. SIRT5 relies on nicotine adenine dinucleotide $(NAD)^+$ Lys deacetylases to regulate key mammalian biological processes. SIRT5-mediated desuccinylation modification has been shown to be involved in the progression of many diseases [15, 16]. However, the role of SIRT5 in chordoma has not been found.

Given this background, this study aimed to explore the effects of SIRT5 on cell proliferation, migration, and invasion and the underlying mechanism in chordoma, which might provide a potential therapeutic intervention strategy for chordoma.

Methods and materials
Bioinformatics analysis
The Search Tool for Recurring Instances of Neighbouring Genes (STRING) database (https://cn.string-db.org/) was used to analyze SIRT5-related proteins. Besides, the GPSuc database (http://kurata14.bio.kyutech.ac.jp/GPSuc/index.php) was used to screen succinylation sites of c-myc.

Sample collection
This study was approved by BeiJing ChaoYang Hospital. The study included 26 patients diagnosed with chordoma. The complete clinical data of chordoma patients, including age, sex, tumor location, tumor size, whether they were primary tumor, and whether the tumor was totally resected were collected in Table 1. The tumor tissue specimens and corresponding adjacent ones (about 2 cm away from the tumor margin) were collected and stored in liquid nitrogen for use. All subjects consented to clinical examination and sampling. Written informed consent was obtained from all subjects.

Cell culture
Chordoma cell lines (U-CH1 and U-CH2), human embryonic kidney (HEK)-293T cells, and human umbilical vein endothelial cells (HUVEC) were purchased from American type culture collection (Manassas, VA, USA). U-CH1 and U-CH2 cells were cultured in Iscove's modified Dulbecco's medium (IMDM)/Roswell Park Memorial Institute (RPMI) (4:1; Gibco; Thermo Fisher Scientific, Inc., Waltham, MA, USA) medium supplemented with 10% heat inactivated fetal bovine serum (FBS, Gibco), 100 U/mL penicillin and 100 μg/mL streptomycin [17]. HEK-293T and HUVEC cells were maintained in Dulbecco's modified eagle medium (DMEM, Thermo Fisher) containing 10% FBS and 1% penicillin/streptomycin. All cells were incubated in a humidified incubator at 37 °C with 5% CO_2.

Cell transfection
SIRT5 short hairpin (sh) RNA (sh-SIRT5), negative control shRNA (sh-NC), negative control pcDNA 3.1 vector, and pcDNA 3.1-c-myc overexpression vector were synthesized by GenesScript Biotechnology Co. Ltd. (Nanjing, China). The cells (5×10^5 cells/well) were inoculated in a

Table 1 Association between SIRT5 expression and the clinicopathologic characteristics of patients with chordoma. **SIRT**, sirtuin

Variables	Number	SIRT5 Expression		
		High (*N* = 13)	Low (*N* = 13)	P value
Age (years)				0.4201
> 50	10	4	6	
≤ 50	16	9	7	
Sex				0.2162
Male	17	7	10	
Female	9	6	3	
Tumor location				0.1847
Skull base	7	5	2	
Spine	19	8	11	
Tumor size				0.6914
≤ 3 cm	11	6	5	
> 3 cm	15	7	8	
Primary tumor				0.0271
Yes	19	12	7	
No	7	1	6	
Total resection				0.6188
Yes	5	2	3	
No	21	11	10	

6-well plate (Corning, NY, USA) a few days before transfection. After the cell confluence reached about 60–80%, transfection was performed using Lipofectamine 3000 (Thermo Fisher) for 48 h. Next, reverse transcription-quantitative polymerase chain reaction (RT-qPCR) was performed to analyze the expression of SIRT5 and c-myc.

In addition, arginine (R) mutations were introduced at K369 (K369R), K385 (K385R) and K411 (K411R) sites of c-myc, respectively (Genscript). Then, c-myc-K369R, c-myc-K385R, and c-myc-K411R were transfected into HEK-293T cells for 24 h.

Animal study

Animal experiment protocols in this study were approved by the Animal Ethics Committee of BeiJing ChaoYang Hospital according to the Guide for the Care and Use of Laboratory Animals (National Research Council). Twelve male BALB/c nude mice (8 weeks old) with an average weight of 25 g purchased from Oricell Biosciences Co. Ltd. (Guangzhou, China) were housed under specific pathogen free conditions at 25℃ with a 12-h light/dark cycle. The mice were randomly divided into two groups: sh-NC and sh-SIRT5 groups (six mice per group). The mice were subcutaneously injected with U-CH1 cells stably transfected with sh-NC and sh-SIRT5 plasmids (1×10^6 cells/100 μL). The volume of the tumors was measured every week, for four weeks. The tumor size was measured with a caliper and the volume was estimated using the formula: $a \times b^2 / 2$ (a, the longest diameter; b, the shortest diameter). The mice were euthanized using pentobarbital sodium (40 mg/kg, Sigma-Aldrich, St. Louis, MO,USA) after 28 days, and the tumors were harvested, weighed and subjected to immunohistochemistry (IHC).

RT-qPCR

Total RNA from tissues and cells was extracted by TRIzol reagent (Yuanye Biotechnology Co. Ltd., Shanghai, China). Then, RNA was reverse transcribed into cDNA using the HiScript IV RT SuperMix for qPCR (Vazyme Biotechnology Co. Ltd., Nanjing, China), and the qPCR amplification experiment was performed using the ChamQ Universal SYBR qPCR Master Mix (Vazyme) with the reaction conditions: 95 ℃ for 30 s, 40 cycles of 95 ℃ for 10 s, 60 ℃ for 30 s, and a melt curve stage. Primers used in this study are synthesized by Tsingke Biotechnology Co. Ltd. (Beijing, China) and listed as follows: sirtuin (SIRT)5, forward, 5′-GCCATAGCCGAGT GTGAGAC-3′ and reverse, 5′-CAACTCCACAAGAGG TACATCG-3′; c-myc, forward, 5′-TCAAGAGGCGAAC ACACAAC-3′ and reverse, 5′-TAACTACCTTGGGGG CCTTT-3′; glyceraldehyde-3-phosphate dehydrogenase (GAPDH), 5′-TGTGGGCATCAATGGATTTGG-3′ and

reverse, 5′-ACACCATGTATTCCGGGTCAAT-3′. The gene expression was calculated by the $2^{-\Delta\Delta CT}$ method.

Western blot

The Total Protein Extraction Kit (Solarbio Science & Technology Co., Ltd, Beijing, China) was used to extract the protein from tissues and cells according to the provided instructions. Then, the homogenate was homogenized in an ice bath, shaken (2 h), and centrifuged (12,000 rpm, 20 min) at 4℃. Then, the supernatant was taken and stored at -80℃ for use. Bicinchoninic acid (BCA) method (Solarbio) was used to detect the protein concentration. After that, 50 μg of protein was separated by 10% SDS-PAGE (Sigma) and transferred to the PVDF membrane (Solarbio). The membrane was blocked in 5% skim milk for 1 h in order to remove nonspecific adsorption, and incubated with the primary antibodies (Sigma) overnight at 4 ℃. Then, the secondary antibody (Sigma) was incubated with the membrane for 1 h at room temperature after washing the membrane three times with Tris-buffered saline Tween (TBST, Solarbio). Finally, protein signal detection was performed using an enhanced chemiluminescence solution (Sigma). The specific proteins were visualized using the Odyssey™ Infrared Imaging System (Gene Company Limited, Hong Kong, China). GAPDH expression was used as an internal control to show equal loading of the protein samples. The used antibodies were listed as follows: SIRT5 (Abcam, Cambridge, MA, USA; ab259967; 1/1000), c-myc (Abcam; ab32072; 1/1000), succinyl lysine (PTM Biolabs, Hangzhou, China; PTM-401; 1/1000), glyceraldehyde 3-phosphate dehydrogenase (GAPDH) (Abcam; ab181602; 1/10,000), and goat anti-rabbit IgG (Abcam; ab205718; 1/5000).

Cell counting kit-8 (CCK-8) assay

Cell viability was detected by the CCK-8 kit (Vazyme) according to the instructions. Three replicate wells were set up. Firstly, the cells were seeded into a 96-well plate (Corning) at the density of 1×10^3 cells/well, then maintained in the incubator for 24 h. After that, 10 μL of CCK-8 solution was added to each well and incubated with cells for 2 h. Finally, a microplate reader (Thermo Fisher) was used to assess the absorbance at 450 nm.

Colony formation assay

For colony formation detection, the cells were planted in 6-well plates and cultured at 37 ℃ for two weeks. Then, the cells were fixed with 4% paraformaldehyde (PFA, Sigma) and stained with 0.5% crystal violet (Solarbio). Finally, the stained cells were counted under a microscope (Olympus, Tokyo, Japan).

Jiang *et al. BMC Cancer*   (2024) 24:386

Page 4 of 10

Transswell migration and invasion assays

The Transswell migration and invasion assays were performed as previously described [18]. For the migration assays, the cells (5×10^4/100 μL) were seeded onto the 24-well Transswells (Corning) uncoated with Matrigel. For the invasion assays, the cells (5×10^4/100 μL) were seeded onto the 24-well Transswells pre-coated with 100 μL of Matrigel. The U-CH1 and U-CH2 cells were resuspended in serum-free medium and added to the upper chamber. The bottom chamber was prepared using 800 μL of RPMI-1640 supplemented with 10% FBS as a chemoattractant. After 48 h of incubation, the cells on the lower surface were washed with phosphate buffer solution (PBS, Vazyme), fixed with 4% PFA for 20 min, and stained in a dye solution containing 0.5% crystal violet for visualization. Finally, the cells were counted and photographed under a microscope. All experiments were performed in triplicate.

Co-immunoprecipitation (Co-IP) assay

Co-IP assay was performed to detect the interaction relationship between SIRT5 and c-myc in HEK-293T cells. After washing by pro-cooled PBS twice, the cells were lysed in Radio Immunoprecipitation Assay Lysis buffer (RIPA) buffer (Vazyme) containing protease inhibitors on ice for 30 min. Then, the supernatant was collected after centrifugating (12,000 *g*, 10 min), and 10 μL of it was taken as the input group. After that, SIRT5, c-myc, or lgG antibody (2 μg) was added into the remaining supernatant and incubated with protein G Plus-Agarose Immunoprecipitation reagent (Abcam) at 4 °C overnight. IgG was used as a negative control. Next, the beads were washed with lysis buffer four times. Immunoprecipitates were eluted by boiling with 1% (wt: vol) SDS sample buffer (Vazyme) and boiled at 100 °C for 5 min. The protein-protein complexes were subsequently subjected to Western blot. The labeled protein membranes were observed and quantified using the Tanon 5200 system (Shanghai, China). The used antibodies were listed as follows: SIRT5 (Abcam; ab259967; 1/30), GAPDH (Abcam; ab181602; 1/60), c-myc (Thermo Fisher; PA5-85185; 1/500), and goat anti-rabbit IgG (Thermo Fisher; 31,460; 1/1000).

Ubiquitination assay

IP assay combined with Western blot were used to access the succinylation level of c-myc (PTM Biotechnology Co., Ltd, Hangzhou, China) in HEK-293T cells. Briefly, the HEK-293T cell lysates were obtained and immunoprecipitated with c-myc antibody c-myc (Thermo Fisher; PA5-85185; 1/500) and protein A/G agarose, followed by Western blot against ubiquitin.

IHC

Paraffin-embedded tumor tissues were cut into sections (about 5 μm), dewaxed, rehydrated, and treated with 3% H_2O_2, respectively. Then, the sections were treated with 10 mM citrate buffer (Yuanye) and boiled in microwave oven for 3 min to expose the site of the antigen. After cooling to room temperature, the citrate buffer was discarded and the sections were washed by PBS twice. Next, normal goat serum was used to block the sections at 37℃ for 30 min. After that, the sections were incubated with primary antibodies against SIRT5 and c-myc overnight at 4℃, and were then treated with goat anti-rabbit IgG at 37℃ for 30 min. After adding DAB solution (Vazyme), the sections were counterstained using hematoxylin (Vazyme) and blued in 1% ammonia water. Finally, the sections were dehydrated, sealed, and observed under a light microscope (Leica Microsystems Trading LTD., Shanghai, China). The used antibodies were listed as follows: SIRT5 (Abcam; ab259967; 1/100), c-myc (Abcam; ab185656; 1/500), GAPDH (Abcam; ab181602; 1/2000), and goat anti-rabbit IgG (Abcam; ab205718; 1/5000).

Protein stability assessment

The cells were treated with cycloheximide (CHX, 100 μg/mL, Yuanye), and the protein level of c-myc at different time points (0, 8, 16, and 24 h) was analyzed by Western blot.

Statistical analysis

The SPSS 21.0 software was used to analyze data. Data are expressed as mean±standard deviation (SD). Student's t-test was used for comparison between the two groups. One-way analysis of variance (ANOVA) was used for comparison among groups. Statistical analyses were performed using GraphPad Prism software (v8.0.1, GraphPad Software Inc., San Diego, CA, USA). $p < 0.05$ indicates that the difference is statistically significant.

Results

High expression of SIRT5 in chordoma tissues and cells

There are few studies on the posttranslational modification of chordoma. Previous articles have found that the progression of chordoma was regulated by ubiquitination modification [19, 20]. Succinylation is a research hotspot in cancer-related diseases in recent years. However, the effects of succinylation on chordoma have not been researched. In this study, we detected the expression of SIRT5 in normal and tumor tissues. The RT-qPCR and Western blot results indicated that the mRNA and protein levels of SIRT5 were increased in tumor tissues in comparison with the normal ones (Fig. 1A and B). Moreover, as indicated in Table 1, 26 patients were divided into high expression ($n=13$) and low expression ($n=13$) according to the expression of SIRT5, further analysis
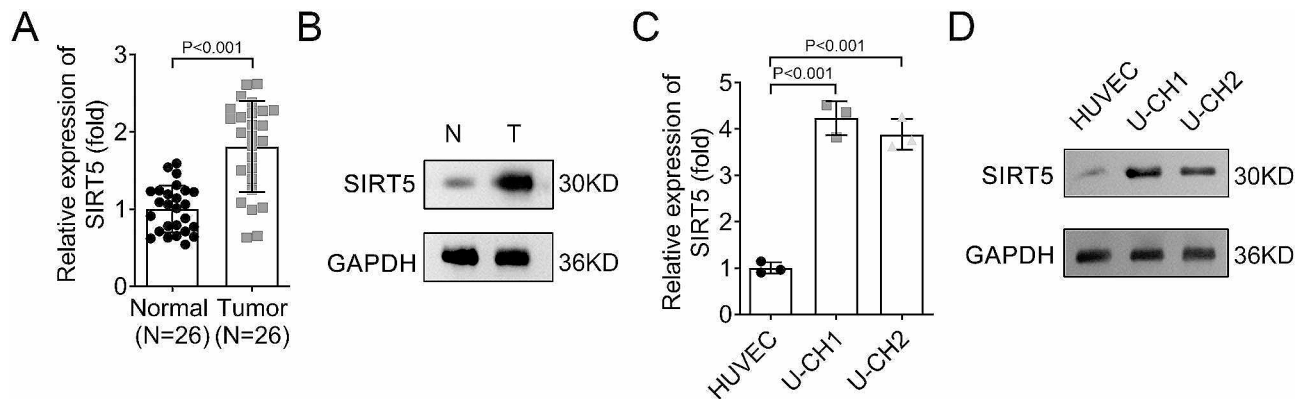
Jiang *et al. BMC Cancer*   (2024) 24:386

Page 5 of 10

Fig. 1 High expression of SIRT5 in chordoma tissues and cells. **A**, RT-qPCR and **B**, Western blot were performed to analyze the mRNA and protein levels of SIRT5 in normal and tumor tissues; The expression of SIRT5 in HUVEC, U-CH1, and U-CH2 cells was analyzed by **C**, RT-qPCR and **D**, Western blot. **SIRT**, sirtuin; **HUVEC**, human umbilical vein endothelial cells; **RT-qPCR**, reverse transcription-quantitative polymerase chain reaction
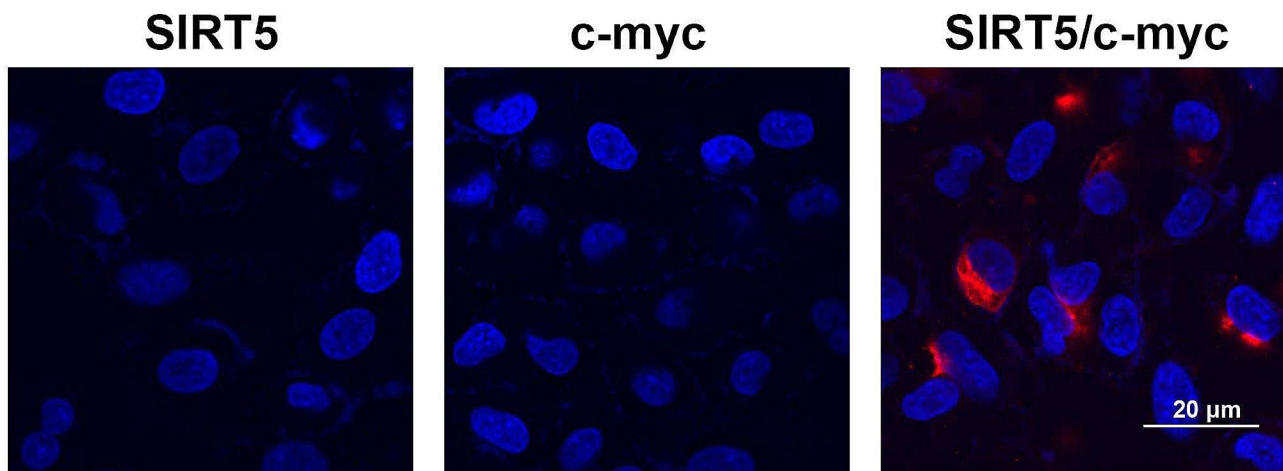
Fig. 2 Knockdown of SIRT5 inhibited cell proliferation, migration, and invasion of U-CH1 and U-CH2 cells. The expression of SIRT5 in sh-NC and sh-SIRT5 groups in U-CH1 and U-CH2 cells was detected by **A**, RT-qPCR and **B**, Western blot; **C**, CCK-8 assay was performed to assess the cell viability of U-CH1 and U-CH2 cells; **D**, Cell colonies were evaluated by colony formation analysis (scale bars = 0.5 cm); **E**, The colony number in sh-NC and sh-SIRT5 groups in U-CH1 and U-CH2 cells; **F**, Transwell assay was performed to detect cell migration (magnification, ×200); **G**, The migration cell number in sh-NC and sh-SIRT5 groups in U-CH1 and U-CH2 cells; **H**, Cell invasion was detected by Transwell assay (magnification, ×200); **I**, The invasion cell number in sh-NC and sh-SIRT5 groups in U-CH1 and U-CH2 cells. **SIRT**, sirtuin; **RT-qPCR**, reverse transcription-polymerase chain reaction; **CCK-8**, cell counting kit-8; **sh-RNA**, short hairpin RNA.

demonstrated that the SIRT5 level was independent of age, sex, tumor location, tumor size, and whether the tumor was totally resected, but correlated with whether the tumor was the primary tumor. In addition, the mRNA and protein levels of SIRT5 in U-CH1 and U-CH2 cells were higher than that in HUVEC cells (Fig. 1C and D).

Knockdown of SIRT5 inhibited cell proliferation, migration, and invasion of U-CH1 and U-CH2 cells

Then, we conducted the in vitro study to explore the role of SIRT5 in chordoma. After transfecting sh-SIRT5 into U-CH1 and U-CH2 cells, the mRNA and protein levels of SIRT5 were downregulated (Fig. 2A and B). The cell viability of U-CH1 and U-CH2 cells was suppressed after SIRT5 inhibition (Fig. 2C). The colony formation and

Transwell assays results showed that the colony number, migration cell number, and invasion cell number were downregulated after SIRT5 inhibition compared with the sh-NC group (Fig. 2D-I). These results suggested that silencing SIRT5 suppressed cell proliferation, migration, and invasion in chordoma.

SIRT5 interacted with c-myc to inhibit the succinylation of c-myc at K369 site

After silencing SIRT5 in HEK-293T cells, the protein level of succinylation was increased (Fig. 3A). STRING database was used to screen SIRT5-associated proteins (Fig. 3B). A previous study has indicated that SIRT5-dependent genes include the c-myc proto-oncogene [21]. Thus, we assessed the interaction between SIRT5 and
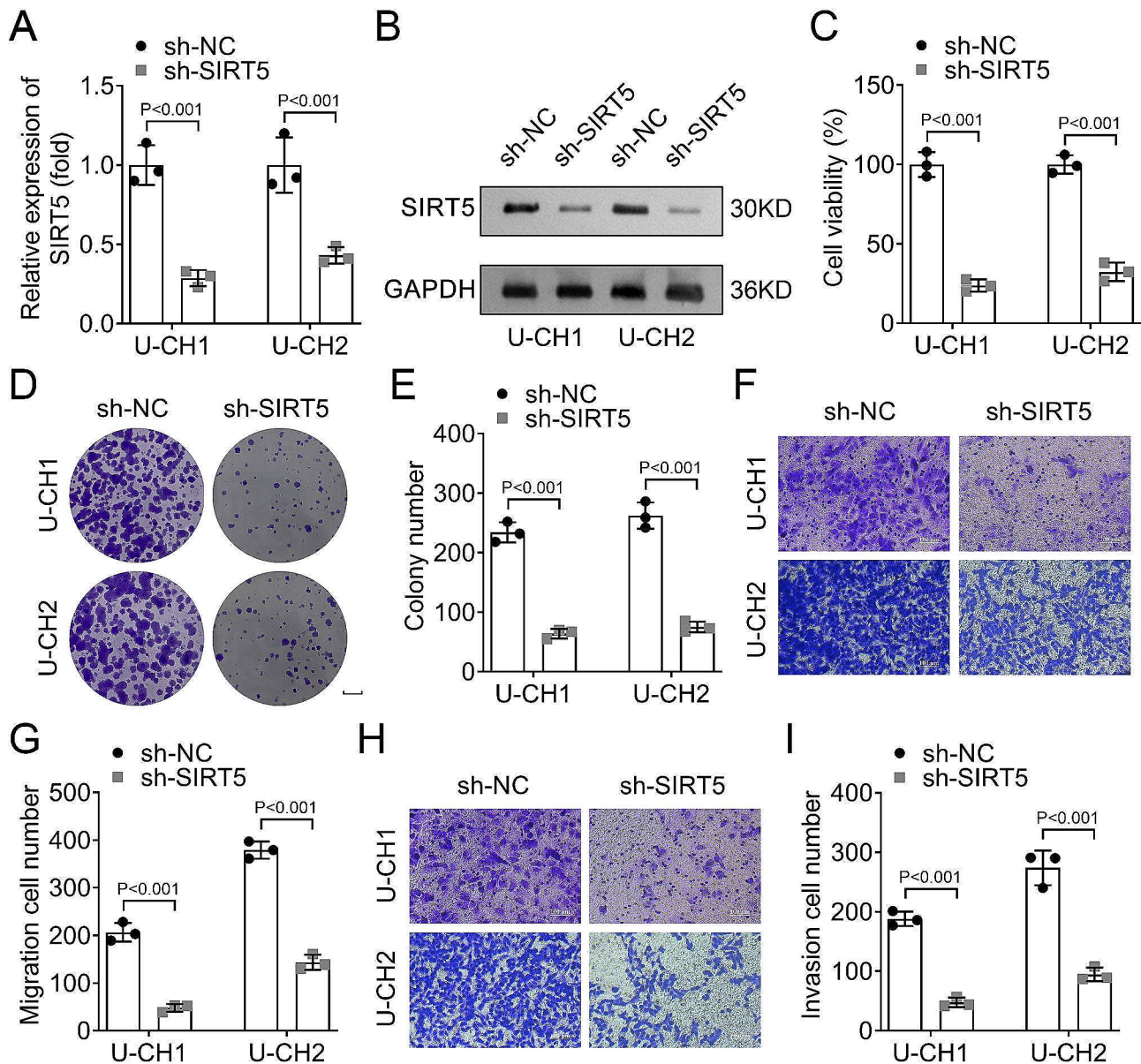
Jiang *et al. BMC Cancer*   (2024) 24:386

Page 6 of 10

Fig. 3 SIRT5 interacted with c-myc to inhibit the succinylation of c-myc at K369 site. **A**, The succinylation level in sh-NC and sh-SIRT5 groups in HEK-293T cells was assessed by Western blot; **B**, STRING database was used to screen SIRT5-related proteins; **C**, Co-IP assay was performed to detect the interaction between SIRT5 and c-myc; **D**, The protein levels of c-myc and c-myc-succ in HEK-293T cells were detected by IP and Western blot after SIRT5 knockdown; **E**, The succinylation sites for c-myc were predicted using GPSuc database; **F**, IP and Western blot assays were used to analyze the succinylation sites of c-myc; **G**, The protein expression of c-myc was assessed by Western blot at the different time points (0, 8, 16, and 24 h) in HEK-293T cells; **H**, Quantification of the existing c-myc protein level at different time points (0, 8, 16, and 24 h) in HEK-293T cells. **SIRT**, sirtuin; **STRING**, Search Tool for Recurring Instances of Neighbouring Genes; **Co-IP**, co-immunoprecipitation; **succ**, succinylation

c-myc. Co-IP assay results showed that SIRT5 was interacted with c-myc in HEK-293T cells (Fig. 3C). In addition, proximity ligation assay was conducted to further demonstrate the interaction between SIRT5 and c-myc in HEK-293T cells (Supplementary Fig. 1). Besides, inhibiting SIRT5 obviously reduced the protein level of c-myc and increased that of c-myc-succ (Fig. 3D). In order to further identify the succinylation sites of c-myc, we used the GPSuc database for prediction, and the results

showed three possible c-myc succinylation sites, K369, K385, and K411 (Fig. 3E). Then, arginine mutations were introduced at K369, K385, and K411 sites of c-myc. IP and Western blot results showed that arginine mutation of K369 site showed upregulated c-myc protein level and downregulated c-myc-succ protein level (Fig. 3F) rather than K385 and K411 sites, suggesting that c-myc was succinylated at K369 site in HEK-293T cells. Protein stability assay results revealed that inhibition of SIRT5

Jiang *et al. BMC Cancer*   (2024) 24:386

Page 7 of 10

downregulated the protein stability of c-myc in HEK-293T cells (Fig. 3G and H).

Overexpressing c-myc reversed the decreased cell viability, colony number, migration and invasion cell numbers caused by silencing SIRT5 in U-CH1 and U-CH2 cells.

After transfecting c-myc overexpression vector into U-CH1 and U-CH2 cells, the mRNA and protein levels of c-myc were increased (Fig. 4A and B). In rescue experiments, the results showed that silencing SIRT5 decreased the cell viability, colony number, migration, and invasion cell numbers compared with the sh-NC group in U-CH1 and U-CH2 cells. Besides, overexpression of c-myc increased the cell viability, colony number, migration and invasion cell numbers in U-CH1 and U-CH2 cells in comparison with the sh-SIRT5+Vector group (Fig. 4C-I).

Silencing SIRT5 inhibited tumor growth of mice

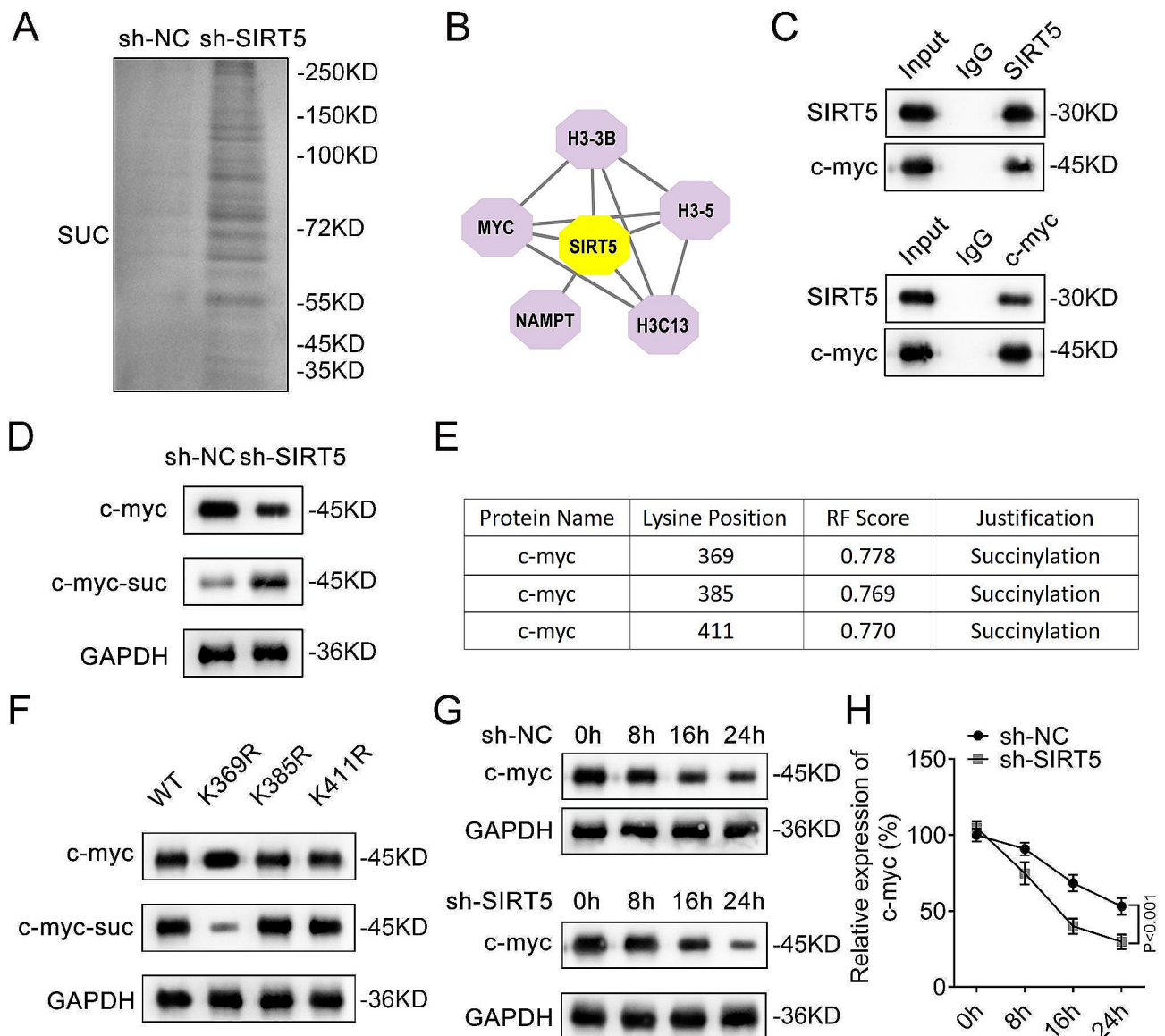The tumor size, weight and volume were suppressed in the sh-SIRT5 group compared with that in the sh-NC

Fig. 4 Overexpressing c-myc reversed the decreased cell viability, colony number, migration and invasion cell numbers caused by silencing SIRT5 in U-CH1 and U-CH2 cells. The expression of c-myc after c-myc overexpression in U-CH1 and U-CH2 cells was detected by **A**, RT-qPCR and **B**, Western blot; **C**, CCK-8 assay was performed to assess the viability of U-CH1 and U-CH2 cells in each group; **D**, Cell colonies were evaluated by colony formation analysis(scale bars = 0.5 cm); **E**, The colony number in each group in U-CH1 and U-CH2 cells; **F**, Transwell assay was performed to detect cell migration (magnification, ×200); **G**, The migration cell number in each group in U-CH1 and U-CH2 cells; **H**, Cell invasion was detected by Transwell assay (magnification, ×200); **I**, The invasion cell number in each group in U-CH1 and U-CH2 cells. **SIRT**, sirtuin; **RT-qPCR**, reverse transcription-polymerase chain reaction; **CCK-8**, cell counting kit-8; **sh-RNA**, short hairpin RNA.

Jiang *et al. BMC Cancer*   (2024) 24:386

Page 8 of 10

group (Fig. 5A-C). IHC assay showed that the protein levels of SIRT5 and c-myc were lower in the sh-SIRT5 group than that in the sh-NC group (Fig. 5D and E).

Discussion

The notochord is thought to be an axial skeleton of primitive structure that promotes the development of surrounding tissues in the early embryo [22]. Chordoma is a rare mesenchymal malignancy with a high recurrence rate, and its tumorigenic mechanism remains unclear. Previous studies have found that genetic alterations, epigenetic regulators, and chromatin spatial organization play crucial roles in the development and progression of chordoma [23]. However, the role of post-translational modification of proteins in chordoma is rarely studied. Succinylation modification has been shown to play key roles in other bone-related diseases, including compression-induced intervertebral disc [15] and early osteoarthritis [24]. However, no study has investigated the effect of succinylation on the development of chordoma. In this study, we found that SIRT5 was increased in chordoma tissues and cells. SIRT5 is the only known desuccinylase [25]. Besides, we found that silencing SIRT5 inhibited proliferation, migration, and invasion of chordoma cells, indicating that SIRT5 promoted malignant advancement of chordoma. Similarly, a previous study demonstrates that SIRT5 deletion promotes obesity-associated osteoarthritis development [24]. In addition, the role of other members of the SIRT family in bone-related diseases has also been described [26, 27]. Interestingly, we found that low level of SIRT5 was also associated with tumors that are not primary chordoma (6 out of 13), suggesting that other primary tumors may have a low level of SIRT5 or that other primary tumors may have a high level of SIRT5 while the SIRT5 level was decreased when progressing and metastasizing.

Additionally, we used HEK-293T cells to further explore the mechanism by which SIRT5 affected the progression of chordoma. The results found for the first time that SIRT5 inhibited the succinylation of c-myc. Similar with our result, a previous study has showed that c-myc is a SIRT5-dependent gene in melanoma [21]. C-myc is located on human chromosome 8, participates in various physiological process, such as cell cycle progression, proliferation and apoptosis [28]. Besides, c-myc is a vital oncogenic transcription factor and closely associated with the progression of different tumor-related diseases [29, 30]. Interestingly, our results also found that c-myc was succinylated at K369 site, which has never been reported in previous studies. This could provide a reference for further study to explore the specific mechanism of c-myc in chordoma or other tumor-related diseases. Moreover, further rescue experiments found that overexpression of c-myc reversed the decreases of proliferation,

migration, and invasion by silencing SIRT5 in chordoma cells, further supporting the above results. In in vivo study, we found that SIRT5 inhibition suppressed the growth of mice, which was consistent with clinical and in vitro studies.

In summary, this finding indicated that SIRT5-mediated desuccinylation of c-myc promoted malignant advancement of chordoma, which might provide new ideas for the clinical treatment of chordoma. However, there are still some limitations in this study, such as a small clinical sample size, which will be further explored in future studies.
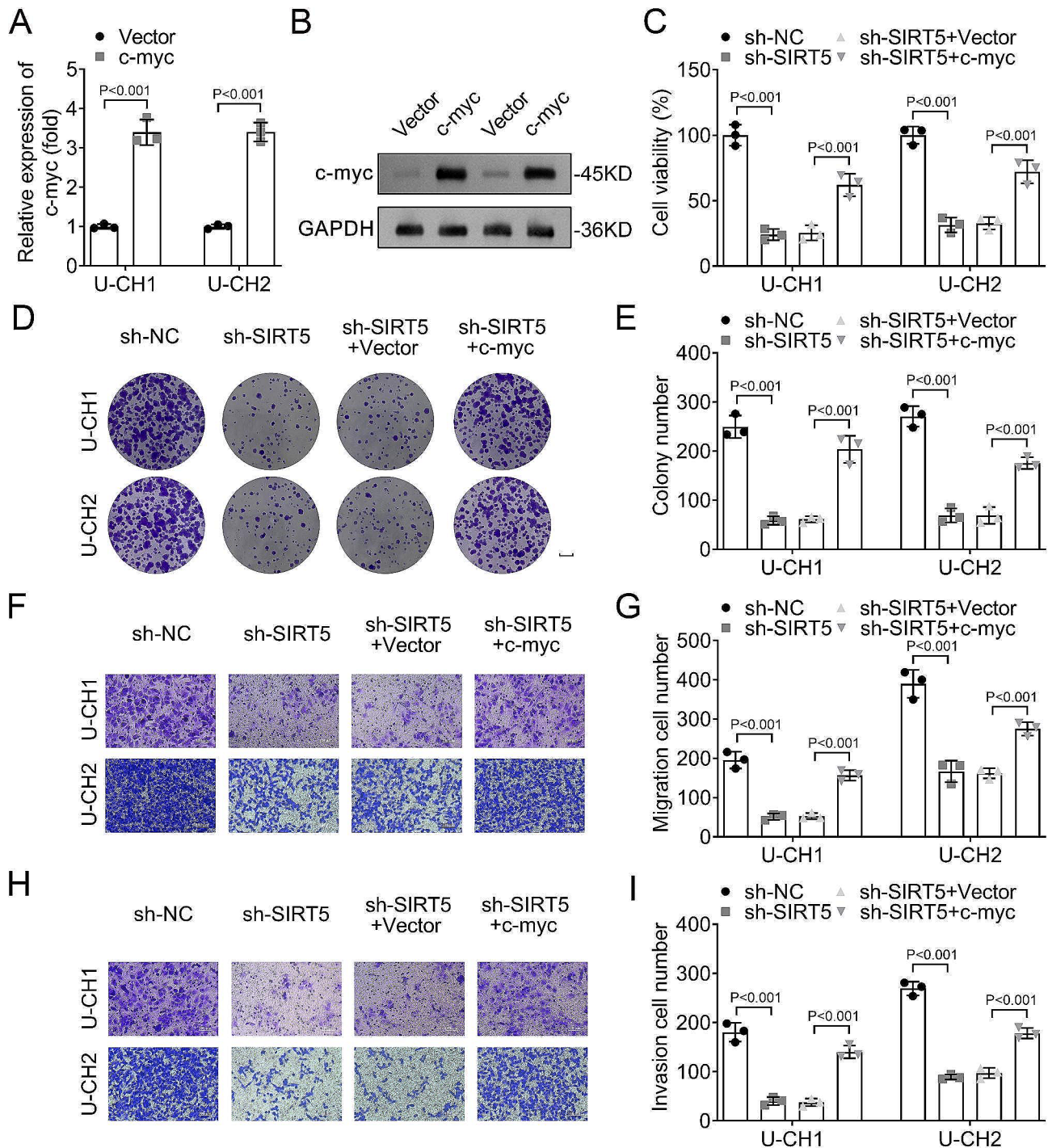
Jiang *et al. BMC Cancer*   (2024) 24:386

Page 9 of 10

Fig. 5 Silencing SIRT5 inhibited tumor growth of mice. **A**, The tumor size, **B**, weight, and **C**, volume in sh-SIRT5 and sh-NC groups; **D**, IHC assay was performed to assess the SIRT5 and c-myc protein levels in sh-SIRT5 and sh-NC groups (scale bar = 100 µm). **SIRT**, sirtuin; **sh-RNA**, short hairpin RNA; **IHC**, immunohistochemistry

Supplementary Information

The online version contains supplementary material available at https://doi.org/10.1186/s12885-024-12140-w.

Supplementary Material 1

Supplementary Material 2

Supplementary Material 3

Supplementary Material 4

Supplementary Material 5

Supplementary Material 6

Jiang *et al. BMC Cancer*   (2024) 24:386

Page 10 of 10

Data availability
The datasets used and/or analyzed during the current study are available from the corresponding author on reasonable request.

Declarations

Ethics approval and consent to participate
The study was approved by the Ethics Committee of BeiJing ChaoYang Hospital. Written informed consent was obtained from all patients. All experiments were performed in accordance with ARRIVE guidelines.

Consent for publication
Not applicable.

Competing interests
The authors declare no competing interests.

References
1. Stacchiotti S, Sommer J. Building a global consensus approach to chordoma: a position paper from the medical and patient community. Lancet Oncol. 2015;16(2):e71–83.
2. Chugh R, et al. Chordoma: the nonsarcoma primary bone tumor. Oncologist. 2007;12(11):1344–50.
3. McMaster ML, et al. Chordoma: incidence and survival patterns in the United States, 1973–1995. Cancer Causes Control. 2001;12(1):1–11.
4. Jo VY, Fletcher CD. WHO classification of soft tissue tumours: an update based on the 2013 (4th) edition. Pathology, 2014. 46(2): p. 95–104.
5. Noor A, et al. Chordoma: a Case Report and Review of Literature. Am J Case Rep. 2020;21:e918927.
6. Stacchiotti S, et al. Chordoma of the mobile spine and sacrum: a retrospective analysis of a series of patients surgically treated at two referral centers. Ann Surg Oncol. 2010;17(1):211–9.
7. Fuchs B, et al. Operative management of sacral chordoma. J Bone Joint Surg Am. 2005;87(10):2211–6.
8. Yu X, Li Z. Epigenetic deregulations in chordoma. Cell Prolif. 2015;48(5):497–502.
9. Alleyn M, et al. The dawn of succinylation: a posttranslational modification. Am J Physiol Cell Physiol. 2018;314(2):C228–32.
10. Zhang Z, et al. Identification of lysine succinylation as a new post-translational modification. Nat Chem Biol. 2011;7(1):58–63.
11. Sreedhar A, Wiese EK, Hitosugi T. Enzymatic and metabolic regulation of lysine succinylation. Genes Dis. 2020;7(2):166–71.
12. Dai X, et al. Succinylation and redox status in cancer cells. Front Oncol. 2022;12:1081712.
13. Mu R, et al. Role of succinylation modification in thyroid cancer and breast cancer. Am J Cancer Res. 2021;11(10):4683–99.
14. Sadhukhan S, et al. Metabolomics-assisted proteomics identifies succinylation and SIRT5 as important regulators of cardiac function. Proc Natl Acad Sci U S A. 2016;113(16):4320–5.
15. Mao J, et al. SIRT5-related desuccinylation modification of AIFM1 protects against compression-induced intervertebral disc degeneration by regulating mitochondrial homeostasis. Exp Mol Med. 2023;55(1):253–68.
16. Wu S, et al. SIRT5 represses neurotrophic pathways and Abeta Production in Alzheimer's Disease by Targeting Autophagy. ACS Chem Neurosci. 2021;12(23):4428–37.
17. Zhang C, et al. Radioresistance of chordoma cells is associated with the ATM/ATR pathway, in which RAD51 serves as an important downstream effector. Exp Ther Med. 2017;14(3):2171–9.
18. Wei C, et al. Crosstalk between cancer cells and tumor associated macrophages is required for mesenchymal circulating tumor cell-mediated colorectal cancer metastasis. Mol Cancer. 2019;18(1):64.
19. Wang L, et al. DEPDC1B regulates the progression of human chordoma through UBE2T-mediated ubiquitination of BIRC5. Cell Death Dis. 2021;12(8):753.
20. Wang L, et al. Correction to: DEPDC1B regulates the progression of human chordoma through UBE2T-mediated ubiquitination of BIRC5. Cell Death Dis. 2022;13(7):631.
21. Giblin W, et al. The deacylase SIRT5 supports melanoma viability by influencing chromatin dynamics. J Clin Invest. 2021;131(12):e138926.
22. Yamada T, et al. Control of cell pattern in the neural tube: motor neuron induction by diffusible factors from notochord and floor plate. Cell. 1993;73(4):673–86.
23. Meng T, et al. A comparative integrated multi-omics analysis identifies CA2 as a novel target for chordoma. Neuro Oncol. 2021;23(10):1709–22.
24. Liu H, et al. Cellular carbon stress is a mediator of obesity-associated osteoarthritis development. Osteoarthritis Cartilage. 2021;29(9):1346–50.
25. Kumar S, Lombard DB. Functions of the sirtuin deacylase SIRT5 in normal physiology and pathobiology. Crit Rev Biochem Mol Biol. 2018;53(3):311–34.
26. Hu S, Wang S. The role of SIRT3 in the osteoporosis. Front Endocrinol (Lausanne). 2022;13:893678.
27. Chen Y, et al. SIRT1, a promising regulator of bone homeostasis. Life Sci. 2021;269:119041.
28. Dalla-Favera R, et al. Human c-myc onc gene is located on the region of chromosome 8 that is translocated in Burkitt lymphoma cells. Proc Natl Acad Sci U S A. 1982;79(24):7824–7.
29. Swartling FJ. Myc proteins in brain tumor development and maintenance. Ups J Med Sci. 2012;117(2):122–31.
30. Robson S, Pelengaris S. Khan, c-myc and downstream targets in the pathogenesis and treatment of cancer. Recent Pat Anticancer Drug Discov. 2006;1(3):305–26.

Publisher's Note
Springer Nature remains neutral with regard to jurisdictional claims in published maps and institutional affiliations.